00E6727F

Environment Canada

Environnement Canada

National Water Research Institute

Institut National de Recherche sur les Eaux

Inland Waters Directorate

Direction Générale des Eaux Intérieures

CRITICAL MEAN VELOCITY FOR OPEN CHANNEL FLOW OVER COARSE BED MATERIAL

by

Peter Engel

Environmental Hydraulics Section
Hydraulics Division
National Water Research Institute
Canada Centre for Inland Waters

September, 1983

MANAGEMENT PERSPECTIVE

In rivers and water channels with a bed composed of granular material, it is often useful to know the point at which the water flow will just cause the bed particles to move.

Scientifically, this point is reasonably well defined but requires the computation of the bed shear velocity which is difficult to determine with precision in the field. Also, it is a hydraulic concept not entirely familiar to many engineers and sedimentologists.

This paper, therefore, examines the available data to enable the critical mean velocity of flow to be established from measurements of depth and grain size distribution. The author proposes a new equation, similar to others already published, but which may be an improvement. More experimental data is required to either correct the proposed equation, vindicate it or reject it.

The proposed equation should be very useful for many field and engineering investigations.

T. Milne Dick
Chief
Hydraulics Division

PERSPECTIVE DE GESTION

Dans les cours d'eau et chenaux de cours d'eau dont le lit est composé de produits granulaires, il est souvent utile de savoir à quel moment le courant d'eau déplace les particules.

D'un point de vue critique, ce détail est assez bien défini, mais il faut calculer la vitesse de cisaillement du lit, qu'il est difficile de déterminer avec précision sur le terrain. Il s'agit aussi d'une notion d'hydraulique avec laquelle beaucoup d'ingénieurs et sédimentologistes ne sont pas familiarisés.

Dans cet article, on examine, donc les données disponibles pour pouvoir établir la vitesse critique moyenne d'écoulement, d'après des mesures de la profondeur et de la granulométrie. L'auteur propose une nouvelle équation, semblable à d'autres déjà publiées, mais qui représente peut-être déjà une amélioration. Il faut davantage de données expérimentales pour corriger l'équation proposee, la justifier ou la rejeter.

L'équation proposée devrait être très utile pour de nombreuses études techniques et études in situ.

T. Milne Dick
Chef
Division d'hydraulique

SUMMARY

Using dimensional analysis it was shown that the dimensionless critical mean flow velocity is a function only of the relative flow depth when the flow is fully rough turbulent. This made it possible to develop a theoretical equation for the critical flow velocity using the Karman-Prandtl logarithmic velocity distribution. Comparison of this equation with those proposed by others showed that it gave the most reliable estimates of critical flow velocity for all depth to grain size ratios greater than 10. The equation was used to develop a critical velocity diagram which can be used to determine the competent flow velocity when the specific gravity of the bed material is 2.7 which is appproximately the value for most river gravels and coarse sands.

RÉSUMÉ

En faisant appel à l'analyse dimensionnelle, on a démontré que la vitesse moyenne critique d'écoulement, exprimée sans dimension, n'est fonction que de la profondeur relative d'écoulement, lorsque l'écoulement est particulièrement turbulent. On est aussi parvenu à élaborer une équation théorique de la vitesse critique d'écoulement, en employant la distribution logarithmique de la vitesse selon Karman-Prandtl. En comparant cette équation à d'autres proposées, on a vu qu'elle donnait l'estimation la plus fiable de cette vitesse critique à toutes les profondeurs, jusqu'à des rapports granulométriques supérieurs à 10. On a employé cette équation pour établir un diagramme de la vitesse critique qui permette de déterminer la vitesse d'écoulement compétente, lorsque la densité des matériaux du lit est 2,7, soit approximativement la valeur caractérisant la plupart des graviers et sables grossiers fluviatiles.

TABLE OF CONTENTS

	Page
MANAGEMENT PERSPECTIVE	i
SUMMARY	iii
1.0 INTRODUCTION	1
2.0 DIMENSIONAL ANALYSIS	3
3.0 CRITICAL VELOCITY EQUATION	6
3.1 General Form of the Equation	6
3.2 Determination of $\tau_c/\gamma_s D_{50}$ and n	9
3.3 Comparison of Critical Velocity Equation with Experimental Data	10
3.4 Effect of Changes in $\tau_c/\gamma_s D_{50}$ and n	12
3.4.1 Varying $\tau_c/\gamma_s D_{50}$ when n = 2.5	13
3.4.2 Varying n when $\tau_c/\gamma_s D_{50}$ = 0.041	14
3.4.3 Varying $\tau_c/\gamma_s D_{50}$ and n simultaneously	14
3.5 Comparison with Other Critical Velocity Equations	15
4.0 CRITICAL VELOCITY DIAGRAM	20
5.0 CONCLUSIONS	22
REFERENCES	
TABLE	
FIGURES	

1.0 INTRODUCTION

Knowledge of the initiation of sediment transport is important for many hydraulic problems dealing with flows over mobile granular beds. There are basically two ways of looking at the problem: a) considering some average velocity such as mean flow velocity, velocity at the bed or velocity at some given distance above the bed; b) considering the average shear stress exerted on the bed particles by the flow. Velocity criteria were first used by the early investigators. Lelliavsky (1966) quoted data that were first presented by Du Buat in 1816. Fortier and Scobie (1926) presented results for permissible bottom velocities in canals. Hjulström (1935) presented a diagram of critical mean flow velocity as a function of grain diameter over a wide range of sizes from 0.001 mm to 100 mm. This diagram has the disadvantage of not including depth as a parameter, but was widely used and is included in many text books of geology and engineering. A major advance in the determination of beginning of bed material transport was provided by Shields (1936) when he introduced his critical shear stress diagram. The dimensionless shear stress was plotted as a function of the grain size Reynolds number over the smooth, transitional and fully rough turbulent flow regimes. Since the introduction of the Shield's diagram the trend in research has been to abandon velocity criteria in favour of shear stress because the latter is a more satisfactory quantity from a fundamental and experimental point of view. The result has been the production of a large body of data to further define the Shield's curve. The most recent and complete version of this curve was presented by Yalin and Karahan (1979) using available data and results from their own experiments.

In spite of the advantages of the shear stress criterion from a scientific point of view, there are some distinct practical

advantages to the use of the flow velocity criterion. From the point of view of the design engineer, the shear stress is not always the most practical parameter because it is difficult to measure in the field (Neill, 1967). It is equally awkward for geologists, limnologists and oceanographers as they are usually dealing with situations where bed shear stress data are secondary at best (Miller, 1977). For hydraulic design purposes it is therefore most practical to use the mean flow velocity as the variable to define the beginning of bed material transport because it is most easily determined. This variable is then referred to as the critical mean flow velocity. In order for critical velocity data to be reliable it is necessary to be able to precisely determine the point of incipient transport. This can only be done satisfactorily in flumes. At the present time the only available criticial velocity data from flumes are those of Mavis,Ho and Tu (1935), Linton Hydraulics Laboratory (1938), Bogardi and Yen (1938), Meyer-Peter and Müller (1948) and Neill (1967). The disadvantage of flume studies is that the size of bed particles and flow depth are restricted. As a result there is a lack of sufficient data which covers the range of conditions normally encountered in river problems. It would therefore be useful to determine some functional relationship which can be confirmed with the existing laboratory data and extended to provide critical mean flow velocity information for design engineers.

In this report the available experimental data on critical mean flow velocity are re-examined. Advantage is taken of the fact that the mean velocity is related to the shear velocity through basic theoretical relationships, thereby making use of the extensive research that has been made on critical shear stress. The results are used to prepare a design curve for practical hydraulic problems. The design curve is compared with relationships proposed by Straub (1953), Rottner (1959), Neil (1967), Bogardi (1974) and Yalin (1977).

2.0 DIMENSIONAL ANALYSIS

The present analysis is restricted to two dimensional, clear, uniform, tranquil flow over plane beds composed of uniformly sized, granular, cohesionless particles of similar shape. For such a flow the critical mean velocity should be expressed as:

$$U_c = f_1 [U_{*c}, h_c, D_{50}, \rho_s, \rho, \mu, \gamma_s] \quad (1)$$

where:
- U_c = critical mean velocity,
- f_1 = denotes a function,
- U_{*c} = critical shear velocity,
- h_c = critical average depth of the flow,
- D_{50} = median grain size,
- ρ_s = density of the granular material,
- ρ = density of the fluid,
- μ = dynamic viscosity of the fluid, and
- γ_s = specific mass of the bed material.

Using dimensional analysis one obtains the following dimensionless equation:

$$\frac{U_c}{U_{*c}} = f_2 \left[\frac{h_c}{D_{50}}, \frac{\rho_s}{\rho}, \frac{U_{*c} D_{50} \rho}{\mu}, \frac{\rho U_{*c}^2}{\gamma_s D_{50}} \right] \quad (2)$$

After multiplying both U_c and U_{*c} by $\sqrt{\rho}/\sqrt{\gamma_s D_{50}}$ and squaring both sides of equation (2), one obtains the relationship:

$$\frac{\rho U_c^2}{\gamma_s D_{50}} = \frac{\rho U_{*c}^2}{\gamma_s D_{50}} f_3 \left[\frac{h_c}{D_{50}}, \frac{\rho_s}{\rho}, \frac{U_{*c} D_{50} \rho}{\mu}, \frac{\rho U_{*c}^2}{\gamma_s D_{50}} \right] \quad (3)$$

The dimensionless critical mean velocity in equation (3) in general, for the conditions specified, depends on the given four dimensionless independent variables. However, several of these can be omitted by the following reasoning. For the present considerations the flow is always in the fully rough turbulent regime. Therefore, there cannot be any effects due to fluid viscosity and the Reynolds number $U_{*c}D_{50}\rho/\mu$ may be omitted from equation (3). In this flow regime the value of $\rho U_*^2/\gamma_s D_{50}$ is known to be constant (Yalin and Karahan, 1979) and hence may also be removed as an independent variable. Finally, at the point of beginning of bed material transport the specific gravity should also be of no significant consequence (Yalin, 1977). Therefore, after taking square roots on both sides the critical velocity can now be written in the reduced form of:

$$\frac{\sqrt{\rho}U_c}{\sqrt{\gamma_s D_{50}}} = f_4\left[\frac{h_c}{D_{50}}\right] \qquad (4)$$

Equation (4) shows that the dimensionless critical mean flow velocity should only depend on the relative depth to bed material size ratio. This is in contrast to the critical shear stress which in this flow regime is in itself sufficient to define the onset of transport. The depth is required to define the critical mean flow velocity because for the same plane granular bed, having the same bed shear stress, there can be different combinations of velocity and depth.

The available experimental data from Mavis, Ho and Tu (1935), Linton Hydraulics Laboratory (1938), Bogardi and Yen (1938), Meyer-Peter and Müller (1948) and Neil (1967) were used to compute values of $\sqrt{\rho}U_c/\sqrt{\gamma_s D_{50}}$ and h_c/D_{50} and these are given in Table 1.

Values of $\sqrt{\rho}U_c/\sqrt{\gamma D_{50}}$ were plotted versus $\ln(h_c/D_{50})$ in Figure 1. The plot shows that there is a general increase in $\sqrt{\rho}U_c/\sqrt{\gamma_s D_{50}}$ as h_c/D_{50} increases. However, the data extend only

over a limited range of h_c/D_{50} from about 5 to 100 and exhibit considerable scatter. The scatter is primarily due to the difficulty and lack of uniformity in the criteria used to determine the point of incipient transport at which U_c and h_c are measured. Yalin (1977) has shown that in order for different observers to obtain similar results from experiments on a series of plane beds, each composed of grains of the same shape but of different grain sizes, the following conditions must be specified:

$$m = \text{constant} \tag{5}$$

$$A/D^2 = \text{constant} \tag{6}$$

$$t\sqrt{\frac{\gamma_s}{\rho D_{50}}} = \text{constant} \tag{7}$$

where: m = the number of grains observed,
A = the surface area of the bed, and
t = the time over which the "m" particles are counted.

The above criteria show that one can never really observe the instant of beginning of bed movement (i.e., zero motion), but only some small rate of transport, the magnitude of which must be decided upon.

None of the data in Figure 1 were obtained using any similitude criteria indicated by equations (5), (6) and (7). As a result, these data, although they show a trend, are not reliable enough by themselves to define a relationship between $\sqrt{\rho}U_c/\sqrt{\gamma_s D_{50}}$ and h_c/D_{50}. However, additional insight into the relationship can be obtained by making use of the logarithmic velocity distribution and available information on the critical shear stress as defined by the well known "Shield's" curve.

3.0 CRITICAL VELOCITY EQUATION

3.1 General Form of the Equation

The von Karman-Prandtl equation for the velocity distribution near a rough boundary is of the form:

$$U_y = \frac{U_*}{\kappa} \ln\left(\frac{y}{k_s}\right) + c \qquad (8)$$

in which U_y = velocity at a distance of y from the boundary, κ = von Karman constant, y = the distance above the bed of the channel, k denotes the height of the boundary roughness and c is a constant of integration. An expression for the mean flow velocity can be obtained from:

$$U = \frac{\int_{k_s}^{h} U_y dy}{(h-k_s)}$$

which results in the relationship:

$$U = \frac{U_*}{\kappa}\left[\ln\left(\beta/e\right) + \frac{\ln\left(\frac{h}{k_s}\right)}{\left(1 - \frac{k_s}{h}\right)}\right] \qquad (10)$$

in which U = mean velocity of the flow, β is a coefficient which is related to the coefficient c in equation (8) by the relationship $\beta = e^{\kappa c}$, and e is the base of natural logarithms. For a clear flow the value of $\kappa = 0.40$. Also, Nickuradse (1933) has shown that for a fully rough turbulent flow c = 8.5 and therefore $\beta = 30.1$. Nikuradse's

experiments were conducted with flows thorugh pipes roughened with tightly packed sand grains of uniform size and consistent rounded shapes. The diameter of the grains was taken as the roughness height which is normally denoted by k_s. Equation (10) may now be written as:

$$U = U_* \left[6.0 + 2.5 \frac{\ln\left(h/k_s\right)}{\left(1 - k_s/h\right)} \right] \tag{11}$$

in which $2.5 \ln\left(\frac{30.1}{e}\right) = 6.0$.

For the condition of critical shear stress in rough turbulent flow it is known that:

$$\frac{\tau_c}{\gamma_s D_{50}} = \text{constant} \tag{12}$$

where τ_c = critical shear stress, The critical shear stress can now be incorporated into equation (11) by noting that $U_* = \sqrt{\tau/\rho}$. After some algebraic manipulation one may now write the critical mean flow velocity as:

$$\frac{\sqrt{\rho}U_c}{\sqrt{\gamma_s D_{50}}} = \frac{\sqrt{\tau_c}}{\sqrt{\gamma_s D_{50}}} \left[6.0 + \frac{2.5}{\left(1 - \frac{k_s}{h_c}\right)} \ln\left(\frac{h_c}{k_s}\right) \right] \tag{13}$$

It can be shown from dimensional consideration that in general, for a plane granular bed, the dimensionless equivalent sand grain roughness should be expressed as:

$$\frac{k_s}{D} = \phi(\Omega, \Theta, \Psi) \tag{14}$$

where ϕ denotes a function, Ω = the areal concentration of the grains, Θ = a factor characterizing the geometric properties of the grains and Ψ = grain size distribution factor such as D_{84}/D_{16}. For a granular plane bed the concentration is virtually constant and therefore Ω is not important. For most river bed material the particles are quite rounded from abrasion and on average may be considered to be quite similar. As a result the parameters Θ may also be removed from further consideration. Finally, although no data are available, one would expect that k_s/D should vary with changes in Ψ. However, for the uniform or near uniform materials considered here, this parameter should also have only a small effect. Therefore for the present consideration one may use the simplified case of equation (14) using D_{50} as the characteristic grain size, given as:

$$\frac{k_s}{D_{50}} = n = \text{constant} \tag{15}$$

Substituting equation (15) into equation (13) the final general equation for the critical mean flow velocity becomes:

$$\frac{\sqrt{\rho}U_c}{\sqrt{\gamma_s D_{50}}} = \frac{\sqrt{\tau_c}}{\sqrt{\gamma_s D_{50}}} \left[6.0 + \frac{2.5}{1 - \left(\frac{nD_{50}}{h_c}\right)} \ln\left(\frac{h_c}{nD_{50}}\right) \right] \tag{16}$$

Equation (16) is similar to equation (4) but has the distinct advantage that the functional dependence has been made explicit by the use of the logarithmic velocity distribution and the relationship between k_s and D_{50}. The equation is valid for all values of h_c/nD_{50} greater

than about 4 (Bayazit, 1975). For values of h_c/nD_{50} less than 4, the logarithmic velocity profile on which equation (16) is based is not valid. The accuracy in determining $\sqrt{\rho}U_c/\sqrt{\gamma_s D_{50}}$ depends on the values of the Shield's parameter $\tau_c/\gamma_s D_{50}$ and n both of which must be obtained from experimental data.

3.2 Determination of $\tau_c/\gamma_s D_{50}$ and n

The value of $\tau_c/\gamma D_{50}$ for the rough turbulent flow regime can be obtained from the curve in Figure 2 which shows the Shield's parameter $\tau_c/\gamma_s D_{50}$ as a function of the grain size Reynolds number $U_*/D_{50}/\nu$ in which ν = kinematic viscosity. This curve represents the best estimate of the critical shear stress parameter at the present time and is based on the most reliable available data. The curve shows that $\tau_c/\gamma_s D_{50}$ is constant at a value of 0.041, which gives a value of $\sqrt{\tau_c}/\sqrt{\gamma_s D_{50}} = 0.202$ for equation (16).

Nikuradse (1933) assumed for his experiments that n = 1. However, experimenters have since then found that in fact n > 1. This difference is not easily explained, but may partly be due to the method of gluing down the grains used by Nikuradse (Kamphuis, 1974; O'Loughlin and MacDonald, 1964). This observation seems to be supported by the fact that there was no difference in the average value of n obtained by Kamphuis (1974) with glued down grains and Bishop, as given by Yalin (1977), for the case of a loose surface layer of a granular medium. Schlichting (1937) obtained a value of n = 1.64 for a single case of a uniform sand grain roughness in a rectangular conduit. O'Laughlin and MacDonald (1964) found that for sand grains glued to a flat boundary at maximum concentration (i.e., similar to the closed packed grains used by Nikuradse (1933)), n = 1.51. Kamphuis (1974) conducted similar experiments and for his data a value

of n = 2.2 can be obtained. Finally, Yalin (1977) reported some data obtained by Bishop for which the average value of n was approximately 2. Taking the average of these values one obtains n = 1.8. However, considering the uncertainty in the determination of n from experimental measurements, a value of n = 2 may be taken as a representative value for a bed of uniform granular material.

3.3 Comparison of Critical Velocity Equation with Experimental Data

The values of $\sqrt{\tau_c}/\sqrt{\gamma_s D_{50}}$ = 0.202 and n = 2 were substituted into equation (16) to yield:

$$\frac{\sqrt{\rho}U_c}{\sqrt{\gamma_s D_{50}}} = \left[1.215 + \frac{0.506}{\left(1 - \frac{2D_{50}}{h_c}\right)} \ln\left(\frac{h_c}{2D_{50}}\right)\right] \qquad (17)$$

Equation (17) was plotted in Figure 3 as $\sqrt{\rho}U_c/\sqrt{\gamma_s D_{50}}$ vs. $\ln(h_c/D_{50})$. The curve is linear for values of $h_c/D_{50} > 15$. For values of $h_c/D_{50} < 15$ the equation becomes slightly non linear, curving slightly in the direction of increasing $\sqrt{\rho}U_c/\sqrt{\gamma_s D_{50}}$. This is a direct result of the effect of the quantity $(1 - 2D_{50}/h_c)$ in equation (17) because as h_c/D_{50} becomes smaller, the term $2D_{50}/h_c$ becomes increasingly more significant.

The data from Table 1 were then plotted for comparison with equation (17). The plot shows, similar to that in Figure 1, an increase in the dimensionless critical velocity with an increase in h_c/D_{50}. Although the trend of equation (17) follows the general trend of the plotted data quite well, the relative position of the curve is too high. The reason for this must lie in the choice of either $\tau/\gamma_s D_{50}$ or n or possibly both.

As pointed out in Section 3.2, $\tau_c/\gamma_s D_{50}$ is obtained from Figure 2 which represents the result of a review of the best available data. It is felt, therefore, that the chosen value of $\tau_c/\gamma_s D_{50}$ = 0.041, is very close to being correct. Therefore, the discrepancy in equation (17) is most likely due to the adopted value of n = 2. This may be due to the following reason. At the time that U_c is measured, there is some particle movement. As a result, because isolated particles are removed from their position of rest, thereby becoming fully exposed and at the same time creating extra depressions at the places once occupied by them, additional roughness is created which provides an increase in surface resistance. Colebrook and White (1937) found that addition of only a small number of larger grains to a surface covered uniformly with smaller grains increased the equivalent roughness size by as much as 50%. It seems, therefore, logical that for the critical case of bed movement there should be some increase in the equivalent sand grain roughness which is reflected by an increase in the value of n. Equation (16) was, therefore, replotted to provide an average fit to the bulk of the data in Figure 3 by trial and error. This resulted in a value of n = 2.5, which agrees with the value determined by Engel (1983). In fitting the equation for n = 2.5 to the bulk of the data, it became evident that the data for Mavis et al (1935) and all but three points on the data from Meyer-Peter and Müller (1948) fell consistently below the plotted curve. The reason for this may lie in the general method of observing the beginning of bed movement. Yalin (1977) has suggested that in general, data for smaller grain sizes are biased towards lower values of critical shear stress because the areas of the beds under observation and the times for which they are observed are not proportional to the square of the diameter of the grains under observation. In other words, observers have not adhered to the necessary conditions given by equations (5), (6) and (7). The grain sizes for the data from Mavis et al (1935) and

Meyer-Peter and Müller (1948) were smaller than that of the other data in Figure 3 and hence are probably most affected by this experimental error, resulting in the relatively low values of $\sqrt{\rho}U_c/\sqrt{\gamma_s D_{50}}$. It is interesting to note, however, that the general trend of the data from Mavis et al and Meyer-Peter and Müller follows the slope of the plotted curve, thus lending further support to the correctness of the basic form of the critical velocity equation. Therefore, adopting the value of n = 2.5 the equation may now be written as:

$$\frac{\sqrt{\rho}U_c}{\sqrt{\gamma_s D_{50}}} = \left[1.215 + \frac{0.506}{\left(1 - \frac{2.5\ D_{50}}{h_c}\right)} \ln\left(\frac{h_c}{2.5\ D_{50}}\right)\right] \qquad (18)$$

Equation (18) is applicable for all values of $h_c/D_{50} \geq 10$. Further, experiments should be conducted to confirm equation (18) for values of $h/D_{50} > 40$ taking care to incorporate the conditions specified by equations (5), (6) and (7) or their equivalents.

3.4 Effect of Changes in $\tau_c/\gamma_s D_{50}$ and n

Equation (18) is a special case of equation (16) in which the values of $\tau_c/\gamma_s D_{50} = 0.041$ and n = 2.5 have been applied. Although both of these values are based on considerable experimental data, it is of interest to see to what degree changes in $\tau_c/\gamma_s D_{50}$ and n can effect the computed critical flow velocity. In order to visualize the effects of such a change, $\sqrt{\rho}U_c/\sqrt{\gamma_s D_{50}}$ in equation (16) was plotted as a function of $\tau_c/\gamma_s D_{50}$ with n as a parameter for the case of $h_c/D_{50} = 100$ in Figure 4. Values of n were taken as n =1, 1.5, 2, 2.5, 3.0 and 4.0.

In general, the effect of $\tau_c/\gamma_s D_{50}$ can be seen in the rate of change of $\sqrt{\rho}U_c/\sqrt{\gamma_s D_{50}}$ as $\tau_c/\gamma_s D_{50}$ increases for each given value of n. The rate of increase in $\sqrt{\rho}U_c/\sqrt{\gamma_s D_{50}}$ is greatest for the lower values of $\tau_c/\gamma_s D_{50}$ and this rate decreases as $\tau_c/\gamma_s D_{50}$ increases for each value of n. The effect of n is felt in two ways. Firstly, it affects the rate of increase in $\sqrt{\rho}U_c/\sqrt{\gamma_s D_{50}}$ as $\tau_c/\gamma_s D_{50}$ increases. The effect is greatest when n = 1 and becomes progressively less as n increases from 1 to 4. Secondly, for a given value of $\tau_c/\gamma_s D_{50}$, the rate of change in $\sqrt{\rho}U_c/\sqrt{\gamma_s D_{50}}$ varies with n, being greatest at low values of n and decreasing rapidly as n increases from 1 to 4.

The region of particular interest in Figure 4 is the shaded area between $\tau_c/\gamma_s D_{50}$ = 0.03 and the often quoted value of $\tau_c/\gamma_s D_{50}$ = 0.05, and between n = 1.5 and n = 3.0. The limits of this shaded area are considered to be representative of the largest likely changes in $\tau_c/\gamma_s D_{50}$ and n, from the adopted values of 0.041 and 2.5, respectively. There are three basic cases of interest. These are: a) varying $\tau_c/\gamma_s D_{50}$ between 0.03 and 0.05 while keeping n constant at 2.5, b) varying n between 1.5 and 3.0 while keeping $\tau_c/\gamma_s D_{50}$ constant at 0.041, and c) varying $\tau_c/\gamma_s D_{50}$ and n simultaneously within their respective stated upper and lower limits.

3.4.1 Varying $\tau_c/\gamma_s D_{50}$ when n = 2.5

If the value of $\tau_c/\gamma_s D_{50}$ were changed from 0.041 to 0.05, there would be an increase in $\sqrt{\rho}U_c/\sqrt{\gamma_s D_{50}}$ of 10.6%. However, decreasing $\tau_c/\gamma_s D_{50}$ to the lower stated limit of 0.03, $\sqrt{\rho}U_c/\sqrt{\gamma_s D_{50}}$ would be reduced by 14.1%. These changes are not excessive and are in keeping with the general magnitude of errors normally associated with mobile boundary problems.

3.4.2 Varying n when $\tau_c/\gamma_s D_{50} = 0.041$

It can be seen from the relative positions of the curves in Figure 4 that the effect of changes in n alone from n = 1.5 to 3.0 is less than the effect of changing $\tau_c/\gamma_s D_{50}$. Figure 4 also shows that the effect of reducing n is greater than the effect of increasing n by the same amount. When n is decreased from 2.5 to 1.5, $\sqrt{\rho}U_c/\sqrt{\gamma_s D_{50}}$ is increased by 9.0%, whereas when n is increased from 2.5 to 3.0, the decrease in $\sqrt{\rho}U_c/\sqrt{\gamma_s D_{50}}$ is only 2.2%. Therefore, possible changes in n alone will not be too serious.

3.4.3 Varying $\tau_c/\gamma_s D_{50}$ and n simultaneously

There are an infinite number of ways that $\tau_c/\gamma_s D_{50}$ and n can be varied simultaneously, within the limits of the shaded region in Figure 4. However, the two cases creating the largest change in $\sqrt{\rho}U_c/\sqrt{\gamma_s D_{50}}$ occur when $\tau_c/\gamma_s D_{50}$ is increased to 0.05 and n is decreased to 1.5; and when $\tau_c/\gamma_s D_{50}$ is decreased to 0.03 and n is increased to 3.0. The first case results in an increase of $\sqrt{\rho}U_c/\sqrt{\gamma_s D_{50}}$ of 20.1% whereas the second case reduces the value of $\sqrt{\rho}U_c/\sqrt{\gamma_s D_{50}}$ by 16.7%. Clearly, the effect of varying $\tau_c/\gamma_s D_{50}$ and n simultaneously is considerably greater than varying them independently. However, the variations in $\tau_c/\gamma_s D_{50}$ and n from the adopted values of 0.041 and 2.5 considered here are larger than is likely to occur in view of the careful review of the available data. Therefore, one can always expect that any errors in computing $\sqrt{\rho}U_c/\sqrt{\gamma_s D_{50}}$ with equation (18) should always be less than 20%. As a result, equation (18) should provide a useful means of computing the critical mean flow velocity for rough turbulent flow over plain, uniform granular beds.

3.5 Comparison with Other Critical Velocity Equations

Other investigators have attempted to obtain relationships for the determination of mean velocity at the point of incipient sediment transport. The five most notable equations which are comparable with the author's equations (i.e., equation (18)) are considered here.

Straub (1953), by considering Shield's critical shear stress criteria used the Manning formula for mean flow velocity together with the Strickler formula to relate Manning's "n" to grain size. This resulted in the equation:

$$U_c = 8.45\left(\frac{\gamma_s}{\gamma}\right)^{1/2}\left(\frac{h_c}{D_{50}}\right)^{1/6} D_{50}^{1/2} \qquad (19)$$

in which γ = specific weight of the fluid. After re-arranging of terms, equation (19) can be written in a dimensionless form compatible with equation (18) as:

$$\frac{\sqrt{\rho}U_c}{\sqrt{\gamma_s D_{50}}} = 1.49\left(\frac{h_c}{D_{50}}\right)^{1/6} \qquad (20)$$

Rottner (1959) analyzed a large volume of data and together with dimensional analysis obtained the relationship:

$$\frac{U_c}{\sqrt{gh_c\left(\frac{\rho_s-\rho}{\rho}\right)}} = \frac{5.53}{\left[\left(\frac{h_c}{D_{50}}\right)^{2/3} + 4.75\right]} \qquad (21)$$

After some re-arranging of terms, equation (21) can be written as:

$$\frac{\sqrt{\rho}U_c}{\sqrt{\gamma_s D_{50}}} = \left(\frac{h_c}{D_{50}}\right)^{1/2} \left[\frac{5.53}{\left(\frac{h_c}{D_{50}}\right)^{2/3} + 4.75}\right] \tag{22}$$

Neill (1967) using dimensional analysis and his own experimental data together with data from other sources, obtained the relationship:

$$\frac{\sqrt{\rho}U_c^2}{\sqrt{\gamma_s D_{50}}} = 2.50 \left(\frac{h_c}{D_{50}}\right)^{0.20} \tag{23}$$

which can be re-arranged into the more compatible form of:

$$\frac{\sqrt{\rho}U_c}{\sqrt{\gamma_s D_{50}}} = 1.58 \left(\frac{h_c}{D_{50}}\right)^{0.10} \tag{24}$$

Bogardi (1974) using his own data and that of other investigators, together with dimensional analysis arrived at the equation:

$$\frac{U_c}{\sqrt{gh_c\left(\frac{\rho_s - \rho}{\rho}\right)}} = 1.7 \left(\frac{h_c}{D_{50}}\right)^{-0.405} \tag{25}$$

After some manipulation of variables, equation (25) can be written as:

$$\frac{\sqrt{\rho}U_c}{\sqrt{\gamma_s D_{50}}} = 1.7 \left(\frac{h_c}{D_{50}}\right)^{0.095} \tag{26}$$

Yalin (1979) using the logarithmic velocity distribution and Shield's critical shear stress criteria obtained the relationship:

$$\frac{\rho U_c^2}{\gamma_s D_{50}} = 0.31 \left[\ln \left(\frac{11.0}{n} \frac{h_c}{D_{50}} \right) \right]^2 \qquad (27)$$

taking square roots on both sides, equation (27) may be written in conformance with the other equations as:

$$\frac{\sqrt{\rho} U_c}{\sqrt{\gamma_s D_{50}}} = 0.56 \ln \left(\frac{11.0}{n} \frac{h_c}{D_{50}} \right) \qquad (28)$$

Yalin considered two values of n, namely n = 1 and n = 2 to define a region between two curves of $\rho U_c^2/\gamma_s D_{50}$ versus h_c/D_{50}. Considering the larger value n = 2, equation (28) can be written as:

$$\frac{\sqrt{\rho} U_c}{\sqrt{\gamma_s D_{50}}} = 0.56 \ln \left(5.5 \frac{h_c}{D_{50}} \right) \qquad (29)$$

Examination of equations (20), (22), (24), (26) and (29) shows that, similar to the author's equation the dimensionless critical mean flow velocity $\sqrt{\rho} U_c/\sqrt{\gamma_s D_{50}}$ is a function only of the dimensionless variable h_c/D_{50}. The equations together with the author's equation are plotted in Figure 5 togethger with the data from Figure 1 as $\sqrt{\rho} U_c/\sqrt{\gamma_s D_{50}}$ versus $\ln (h_c/D_{50})$ for direct comparison.

It can be seen from Figure 5 that for all curves, except that of Rottner, $\sqrt{\rho} U_c/\sqrt{\gamma_s D_{50}}$ continually increases as h_c/D_{50} increases and that there is considerable difference in the shape of the curves. The curves can be separated into two groups, the first group consists of the curves of Straub, Yalin and the author, all of which were obtained with the aid of theoretical methods. The second group consists of the curves of Rottner, Neil and Bogardi, all of

which were developed by fitting curves directly to plotted data. The curves of the first group always give higher values of $\sqrt{\rho}U_c/\sqrt{\gamma_s D_{50}}$ for any hc/D_{50}.

Considering first the curves of the first group, Figure 5 shows that Yalin's curve and the author's are quite similar. For values of $h_c/D_{50} > 1000$, both curves are parallel but when h_c/D_{50} decreases from $h_c/D_{50} \approx 1000$ to $h_c/D_{50} = 10$ there is a continuous decrease in the slope of the author's curve whereas the slope of Yalin's curve remains constant. The reason for this stems from the fact that Yalin let $k_s/h \to o$ when integrating the velocity distribution and the effect of this assumption is felt up to values of $h_c/D_{50} \approx 1000$. Therefore Yalin's curve is only valid for larger values of h_c/D_{50}. The curve of Yalin lies above the bulk of the data and this is due to the fact that he chose a value of the Shield's parameter of $\tau_c/\gamma_s D_{50} = 0.05$ and a value of $n = 2$. Considering the present analysis of the available data and the fact that the author's curve is valid for all values of $hc/D_{50} \geq 10$, the latter should give better results. Straub's curve gives virtually the same values of $\sqrt{\rho}U_c/\sqrt{\gamma_s D_{50}}$ at $hc/D_{50} = 10$ as the author's curve, and for the range of available data fits the data as well as the author's curve. However, as h_c/D_{50} increases above 100, the Straub curve begins to diverge significantly toward larger values. When $h_c/D_{50} = 5000$ values of $\sqrt{\rho}U_c/\sqrt{\gamma_s D_{50}}$ obtained with Straub's curve are about 22% larger than values obtained with the author's curve. Considering that the logarithmic velocity distribution has a sounder theoretical basis than the Manning equation, the author's curve should be more reliable than Straub's curve for values of h_s/D_{50} greater than 100.

The second group of curves demonstrates the risk in extrapolating totally empirical curves far beyond the range of data from which they were developed. The curves of Bogardi (1974) and Neill (1967) are virtually parallel with Bogardi's curve giving slightly higher values of $\sqrt{\rho}U_c/\sqrt{\gamma_s D_{50}}$. The curve of Neill lies along the lower limit of the plotted data because he developed his curve to be the lower envelope to his data set. The curve of Bogardi fits the

plotted data much better because it represents the least squares best fit to his data set which included data for transitional and smooth regime flow which are not included in Figure 5. Considering these facts, the agreement between the curves of Bogardi and Neill is quite good.However, Neill's and Bogardi's curves differ considerably from the author's curve. Although all three curves have comparable values of $\sqrt{\rho}U_c/\sqrt{\gamma_s D_{50}}$ when $h_c/D_{50} = 10$ the rate of increase in $\sqrt{\rho}U_c/\sqrt{\gamma_s D_{50}}$ with h_c/D_{50} for Neil's and Bogardi's curves is much less than that for the author's curve resulting in much lower values of critical mean velocity. However, considering that the author's curve is based on the logarithmic velocity distribution, it should not be less valid as h_c/D_{50} increases beyond the range of the data. Consequently equation (18) should be more reliable than the curve of Neil (1967) and Bogardi (1974). The curve of Rottner gives the lowest value of $\sqrt{\rho}U_c/\sqrt{\gamma_s D_{50}}$ for all values of h_c/D_{50}. The trend of decreasing values of $\sqrt{\rho}U_c/\sqrt{\gamma_s D_{50}}$ as h_c/D_{50} increases for $h_c/D_{50} \geq 70$ is contrary to what could be expected on the basis of physical reasoning and does not agree with the general trend of the experimental data. Therefore, the equation of Rottner should not be used.

In view of the above comparison, the analysis of the latest available data, because of its sound physical basis and its validity for all values of $h_c/D_{50} \geq 10$, the author's curve is considered to be the most reliable tool for estimation of critical mean velocities at the present time.

4.0 CRITICAL VELOCITY DIAGRAM

Equation (18) can be used to prepare a diagram in which the critical velocity U_c can be obtained directly if values of grain size D_{50} and flow depth h_c are known. Such a diagram is useful for direct engineering application while at the same time providing a comprehensive picture of the relative importance of grain size and flow depths. For water flowing over a gravel bed, the specific gravity ρ_s/ρ may be taken on the average as being equal to 2.7. As a result the dependent variable in equation (18) may be reduced for this special case to $U_c/(4.1\sqrt{D_{50}})$ in which $\sqrt{\rho}/\sqrt{\gamma_s} = 4.1$. The critical velocity for gravel beds may then be written as:

$$U_c = 4.1\sqrt{D_{50}} \left[1.215 + \frac{0.506}{1 - \dfrac{2.5\ D_{50}}{h_c}} \ln \frac{h_c}{2.5\ D_{50}} \right] \quad (30)$$

Equation (30) is plotted in Figure 6 as U_c vs. D_{50} with h_c as a parameter for values of h_c = 1 m, 5 m, 10 m and 30 m. Each curve extends from the lower limit of the rough turbulent flow regime at D_{50} = 3 mm to the upper limit of the grain size for which equation (18) is valid. This upper limit was considered to be at the point at which $h_c/D_{50} = 10$ (i.e., $h_c/k_s = 4$) in accordance with findings reported by Bayazit (1975). Figure 6 shows that for a given depth h_c, the critical flow velocity U_c always increases, as well as its rate of change, as the median grain size of the bed D_{50} increases. The rate of change in U_c is least when h_c is small and increases considerably as h_c becomes large. For example, when h_c = 1 m, an increase in D_{50} from 4 mm to 40 mm results in an increase of U_c of 124%. When h_c = 5 m a similar increase in D_{50} increases U_c by 135% and at h_c = 30 mm U_c is increased by 144%.

Figure 6 also shows the effect of depth on U_c for a given value of D_{50}. When D_{50} is constant the rate of increase in U_c decreases as the depth is increased. This effect is least when D_{50} is small and becomes more significant when D_{50} becomes larger. For example, when D_{50} = 4 mm an increase in depth from 1 m to 30 m increases U_c by 50%, whereas when D_{50} = 40 mm a similar increase in depth increases U_c by 64%. This shows that U_c is more sensitive to changes in depths when the bed is composed of larger particles. At the same time, the shape of the curves shows the effect that changes in D_{50} have on the magnitude of the critical velocity. Knowledge of these aspects is important for the design of stable channel cross-sections of canals.

5.0 CONCLUSIONS

5.1 Using dimensional analysis it was shown that the dimensionless critical mean flow velocity $\sqrt{\rho}U_c/\sqrt{\gamma_s D_{50}}$ is a function only of the relative flow depth h_c/D_{50} when the flow is in the rough turbulent flow regime. However, because of limited data and the fact that most data are affected by systematic observational errors, a reliable relationship between the dimensionless critical velocity and the relative depth cannot be obtained at the present time using only dimensional analysis and available data.

5.2 A theoretical equation for the critical flow velocity in terms of relative depth was developed using the universal Karman-Prandtl logarithmic velocity distribution. This approach requires knowledge of the dimensionless critical shear stress at the bed $\tau_c/\gamma_s D_{50}$ (i.e., Shield's parameter) and the relationship between the equivalent sand grain roughness k_s and the representative grain size of the uniform bed given by $n = k_s/D_{50}$. At the present time the most reliable values obtained from experimental data are $\tau_c/\gamma_s D_{50} = 0.041$ and $n = 2.5$. The critical velocity equation is given as:

$$\frac{\sqrt{\rho}U_c}{\sqrt{\gamma_s D_{50}}} = \left[1.215 + \frac{0.506}{\left(1 - \frac{2.5\ D_{50}}{h_c}\right)} \ln\left(\frac{h_c}{2.5\ D_{50}}\right)\right] \qquad (18)$$

The equation is valid for all values of $h/D_{50} \geq 10$ in the rough turbulent flow regime.

5.3 Comparison of equation (18) with that of Straub (1953), Rottner (1959), Neil (1967), Bogardi (1974) and Yalin (1977) showed that it gives the most reliable estimates of critical mean flow

velocity at the present time for all values of critical depth to grain size ratio greater than 10. Equations obtained by fitting curves directly to presently available data tend to grossly under-estimate the critical mean flow velocity for all practival values of critical depth to grain size ratio.

5.4 A critical velocity diagram was developed which can be used to determine the critical flow velocity directly when the specific gravity of the bed material is 2.7, which is the value for most river gravels and coarse sands. The velocity diagram shows directly the effect of depths of flow and grain size on the critical velocity. For a given depth of flow the critical velocity always increases as does the rate of increase, when the grain size is increased. This change in the critical velocity is least when the flow depth is small and increases when the flow depth increases. When D_{50} is constant, the rate of increase in the critical velocity decreases as the depth is increased. This effect is least when the grain size is at the lower limit of the rough turbulent regime (i.e., D_{50} = 3.0 mm) and becomes more significant as the grain size becomes larger.

5.5 Because of the limited range in the existing data on critical mean velocity and its limited value because of observational errors, some tests should be conducted to confirm equation (18) over the range $10 \leq h_c/D_{50} \leq 1000$, before it can be recommended for practical application.

REFERENCES

Bayazit, M., 1975. "Free Surface Flow in a Channel of Large Relative Roughness". Journal of Hydraulic Research, IAHR, Vol. 14, No. 2.

Bogardi, J. and Yen, C.H., 1938. "Traction of Pebbles by Flowing Water. M.Sc. Thesis, University of Iowa.

Bogardi, J., 1974. "Sediment Transport in Alluvial Streams". AKADEMIAI KIADO, Budapest.

Colebrook, C.F.; White, C.M., 1937. "Experiments with Fluid Friction in Roughened Pipes". Proceedings, Royal Society of London, Series A, Vol. 161.

Collins, M.B. and Rigler, J.K., 1982. "The Use of Settling Velocity in Defining the Initiation of Motion of Heavy Mineral Grains Under Unidirectional Flow". Sedimentology (29).

Engel, P., 1983. "Equivalent Roughness of Alluvial Bed". Discussion, submitted to Journal of Hydraulics Division, ASCE.

Falkner, F.H., 1935. "Studies of River Bed Materials and Their Movements with Special Reference to the Lower Mississippi River". U.S. Waterways Experiment Station, January.

Fortier, S. and Scobie, F.C., 1926. "Permissible Canal Velocities". Transactions, ASCE, Vol. 89, Paper No. 1588, pp. 940-984.

Hjulstrom, F., 1935. "Studies of the Morphological Activity of Rivers as Illustrated by the River Fyris.....?". Bulletin, Geological Institute of Upsala, Vol. XXV, Upsala, Sweden.

Iwagaki, Y., 1956. "Hydrodynamical Study on Critical Fractive Force". Transactions, Japan Society of Civil Engineering, No. 41, Tokyo, Japan.

Karahan, E., 1975. "The Determination of the Initiation of the Motionfor Non Uniform Bed Materials". Ph.D. Thesis, Technical University of Istanbul.

Kemphuis, J.U., 1974. "Determination of Sand Roughness for Fixed Beds". Journal of Hydraulics Research, Vol. 12, No. 2.

Kramer, H., 1934. "Sand Mixtures and Sand Movement in Fluvial Models". Proceedings, ASCE, April.

Leliavsky, S., 1966. "An Introduction to Fluvial Hydraulics". Dover Publications Inc., New York.

Linton Hydraulics Laboratory, 1938. Data obtained in Neil (1967).

Mavis, F.T., Ho, C. and Tu, Y.C., 1935. "The Transportation of Detritus by Flowing Water - 1". Bulletin No. 5, University of Iowa, March.

Meyer-Peter, E. and Muller, R., 1948. "Formulas for Bed Load Transport". Proceedings, IHHR Stockholm, June.

Miller, M.C., McCave, I.N. and Komar, P.D., 1977. "Threshold of Sediment Motion Under Unidirectional Currents". Sedimentology, Vol. 24.

Neill, C.R., 1967. "Stability of Coarse Bed Material in Open Channel Flow". Open File Report 1067-8, Research Council of Alberta, Highway Division, Edmonton, Alberta.

Neill, C.R., 1968. "Note on Initial Movement of Coarse Uniform Bed Material". Journal of Hydraulics Research, IAHR, March.

Neill, C.R., Yalin, M.S., 1969. "Quantitative Definition of Beginning of Bed Movement". Journal of Hydraulics Division, ASCE, HY1.

Nikuradse, J., 1933. "Laws of Flows in Rough Pipes". National Advisory Committee for Aeronautics, Technical Memorandum 1292, 1950. Translation of original paper.

O'Loughlin, E.M. and MacDonald, E.G., 1964. "Some Roughness Concentration Effects on Boundary Resistance". La Horville....? Blanche, No. 7.

Rottner, J., 1959. "A Formula for Bed Load Transportation". La Houille Blanche, No. 3, 1959.

Shields, A., 1936. "Anwendung der Ahnlichkeits-mechanik under der Turbulenzforschung auf die Geschiebebewegung". Mitteilungender Preussischen Versuchsanstalt fur Wasserbau und Schiffbau. Heft 26, Berlin.

Schlichting, H., 1937. "Experimentelle Untersuchungen zum..? Rauhrig Keitsproblem". Ingeneur-Archive, Vol. VII, No....? February.

Straub, L.G., 1953. "Dredge-Fill Closure of Missouri River at Fort Randall". Proc. Minnesota Intern. Hydr. Convention (IAHR/ASCE).

White, S.Y., 1970. "Plane Bed Thresholds of Fine Grained Sediments". Nature, Vol. 228, October.

Yalin, M.S., 1977. "Mechanics of Sediment Transport". 2nd Ed., Pergammon Press.

Yalin, M.S. and Karahan, E.M., 1979. "Inception of Sediment Transport". Journal of Hydraulics Division, ASCE, Vol. 105, No. HY11.

TABLE 1. EXPERIMENTAL DATA FOR TRANQUIL FLOW

D_{50} mm	h cm	V_c cm/s	$\frac{\sqrt{\rho}U_c}{\sqrt{\gamma_s D_{50}}}$	$\frac{h_c}{D_{50}}$	$\frac{\rho_s}{\rho}$	Source
2.8	7.8	41.8	1.95	27.7	2.66	Mavis, Ho and Tu (1935)
2.8	9.7	44.5	2.08	34.7	2.66	
2.8	11.1	44.8	2.09	39.5	2.66	
2.8	13.8	54.0	2.52	49.5	2.66	
2.8	17.0	55.8	2.61	60.6	2.66	
4.0	11.2	55.2	2.17	28.0	2.65	
4.0	12.9	57.6	2.27	32.3	2.65	
4.0	16.4	59.7	2.35	41.0	2.65	
5.7	12.3	63.1	2.08	21.7	2.65	
5.7	18.9	72.5	2.39	33.1	2.65	
5.7	20.4	69.5	2.29	35.8	2.65	
5.7	21.6	70.1	2.32	37.9	2.65	
8.0	31.4	103.6	2.85	40.0	2.70	Linnton Hydraulic
11.0	31.7	112.8	2.65	28.6	2.67	Laboratory (1938)
16.0	39.6	134.1	2.63	25.0	2.67	
32.0	55.5	189.0	2.58	17.5	2.72	
10.6	6.8	83.5	2.01	6.4	2.63	Bogardi and Yen (1938)
10.6	5.9	82.6	2.00	5.6	2.63	
10.6	9.9	77.4	1.87	9.4	2.63	
10.6	8.2	78.0	1.87	7.7	2.63	
10.6	10.2	78.0	1.90	9.6	2.63	
10.6	5.52	77.7	1.87	5.2	2.63	
10.6	5.88	83.5	2.02	5.6	2.63	
10.6	7.47	80.2	1.95	7.1	2.63	
10.6	9.20	84.7	2.05	8.7	2.63	
10.6	9.30	87.5	2.12	8.8	2.63	
10.6	10.6	85.6	2.07	10.0	2.63	
10.6	10.5	89.3	2.17	9.9	2.63	
10.6	15.6	96.6	2.32	14.7	2.63	
10.6	16.6	98.8	2.39	15.7	2.63	
5.82	4.4	72.5	2.37	7.5	2.61	
5.82	4.3	73.5	2.39	7.4	2.61	
5.82	10.5	82.3	2.68	18.0	2.61	
5.82	8.51	86.9	2.82	16.3	2.61	

Continued...../

TABLE 1 (Cont'd). EXPERIMENTAL DATA FOR TRANQUIL FLOW

D_{50} mm	h cm	V_c cm/s	$\frac{\sqrt{\rho}U_c}{\sqrt{\gamma_s D_{50}}}$	$\frac{h_c}{D_{50}}$	$\frac{\rho_s}{\rho}$	Source
15.5	8.7	106.0	2.24	5.6	2.64	Bogardi and Yen (1938)
15.5	14.9	106.0	2.12	9.6	2.64	
15.5	15.8	107.0	2.15	10.2	2.64	
3.20	31.3	67.1	2.95	97.8	2.68	Meyer-Peter and Müller
2.70	15.4	57.7	2.76	57.0	2.68	(1948)
3.80	22.9	66.4	2.68	60.3	2.68	
3.60	26.3	69.7	2.88	73.1	2.68	
3.66	13.8	71.7	2.95	37.7	2.68	
8.50	15.4	93.4	2.63	18.1	2.68	
3.66	5.9	60.7	2.49	16.1	2.68	
7.40	7.2	90.6	2.63	9.7	2.68	
8.50	8.4	90.5	2.45	9.9	2.68	
1.86	14.8	49.5	2.85	79.6	2.68	
3.14	22.4	58.6	2.57	71.3	2.68	
3.10	20.4	64.1	2.86	65.8	2.68	
3.66	13.7	70.1	2.88	37.4	2.68	
3.06	12.3	65.0	2.92	40.2	2.68	
2.58	10.5	58.1	2.85	40.7	2.68	
2.61	4.8	57.9	2.81	18.4	2.68	
4.04	7.70	73.1	2.86	19.0	2.68	
6.2	5.19	60.1	2.00	8.4	2.51	
6.2	5.80	67.0	2.20	9.4	2.51	Neill (1967)
6.2	7.0	70.0	2.30	11.4	2.51	
6.2	8.54	71.6	2.35	13.7	2.51	
6.2	8.85	74.6	2.45	14.3	2.51	
6.2	10.0	71.6	2.35	16.3	2.51	
6.2	11.7	74.6	2.45	18.9	2.51	
6.2	13.4	76.2	2.49	21.7	2.51	
6.2	14.6	80.8	2.65	23.6	2.51	
6.2	16.5	70.0	2.30	26.6	2.51	
6.2	19.2	73.1	2.45	31.1	2.51	
8.5	6.01	68.5	1.93	7.2	2.49	
8.5	7.0	64.0	1.79	8.3	2.49	
8.5	9.15	70.0	1.96	10.8	2.49	
8.5	11.0	70.6	1.98	12.8	2.49	

Continued...../

TABLE 1 (Cont'd). EXPERIMENTAL DATA FOR TRANQUIL FLOW

D_{50} mm	h cm	V_c cm/s	$\frac{\sqrt{\rho}U_c}{\sqrt{\gamma_s D_{50}}}$	$\frac{h_c}{D_{50}}$	$\frac{\rho_s}{\rho}$	Source
8.5	12.2	74.7	2.10	14.3	2.49	Neill (1967)
8.5	13.7	83.8	2.35	16.1	2.49	
8.5	15.3	79.3	2.22	17.9	2.49	
8.5	16.8	86.8	2.27	19.6	2.49	
8.5	18.3	74.6	2.10	21.7	2.49	
10.6	6.4	74.6	1.87	6.0	2.51	
10.6	7.93	77.7	1.94	7.5	2.51	
10.6	8.85	80.8	2.02	8.3	2.51	
10.6	10.4	85.4	2.13	9.8	2.51	
10.6	12.2	91.5	2.28	11.5	2.51	
10.6	13.7	90.0	2.25	13.0	2.51	
10.6	15.3	91.5	2.28	14.3	2.51	
10.6	16.8	96.1	2.40	15.9	2.51	
10.6	18.3	94.5	2.36	17.2	2.51	
20.0	14.6	102.0	1.87	7.3	2.49	
20.0	17.4	113.0	2.06	8.7	2.49	
16.0	11.9	106.9	2.20	7.4	2.48	
16.0	14.3	114.2	2.34	8.9	2.48	
16.0	15.9	116.0	2.37	9.9	2.48	
6.4	6.1	29.0	2.08	9.5	1.30	
6.4	7.32	28.4	2.03	11.5	1.30	
6.4	8.85	31.4	2.25	13.9	1.30	
6.4	11.0	32.0	2.29	17.2	1.30	
6.4	12.2	32.0	2.29	19.2	1.30	
6.4	13.4	32.9	2.36	20.8	1.30	
6.4	15.3	34.2	2.45	23.8	1.30	
6.4	16.8	35.0	2.52	26.3	1.30	
6.4	18.3	36.6	2.62	28.6	1.30	
5.0	6.4	56.1	2.08	12.8	2.46	
5.0	7.94	56.4	2.09	15.9	2.46	
5.0	9.75	59.5	2.20	19.6	2.46	
5.0	11.3	63.1	2.34	22.7	2.46	
5.0	12.65	60.1	2.26	25.0	2.46	
5.0	13.7	62.2	2.30	27.5	2.46	
5.0	15.9	65.5	2.43	31.8	2.46	
5.0	17.7	62.5	2.32	35.3	2.46	

F I G U R E S

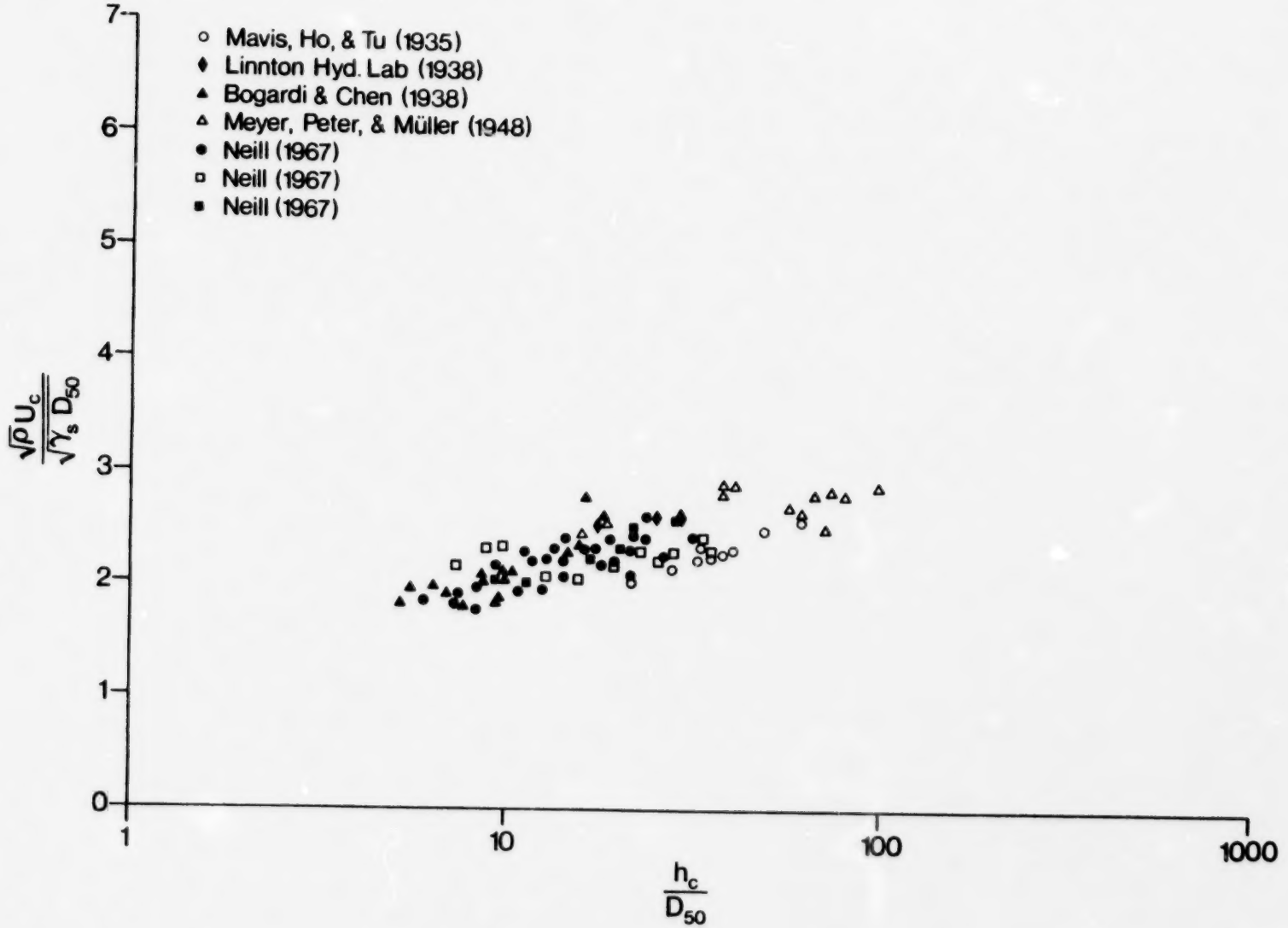

Figure 1

PLOT OF EXPERIMENTAL DATA

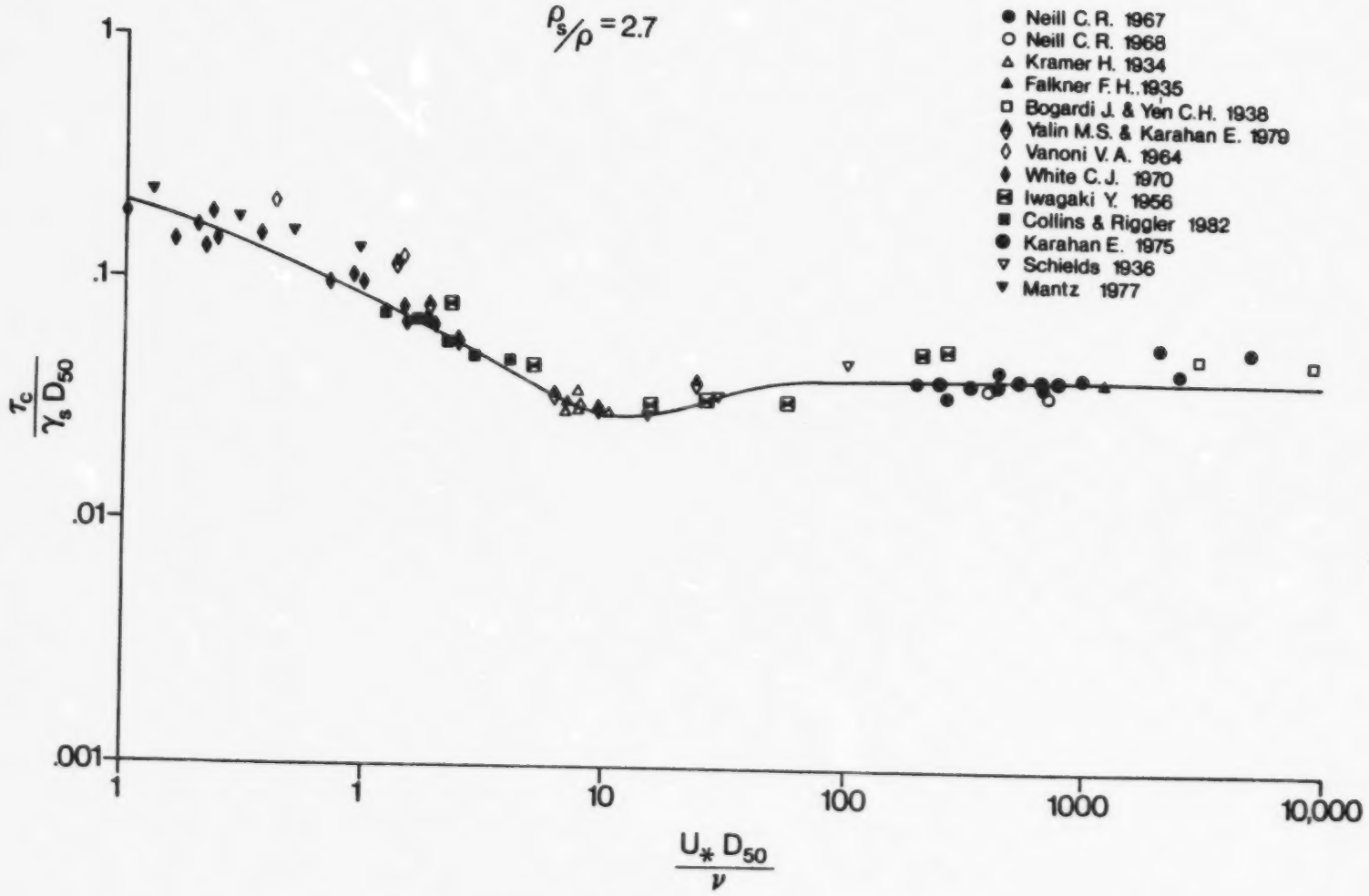

Figure 2 "SHIELD'S" CURVE

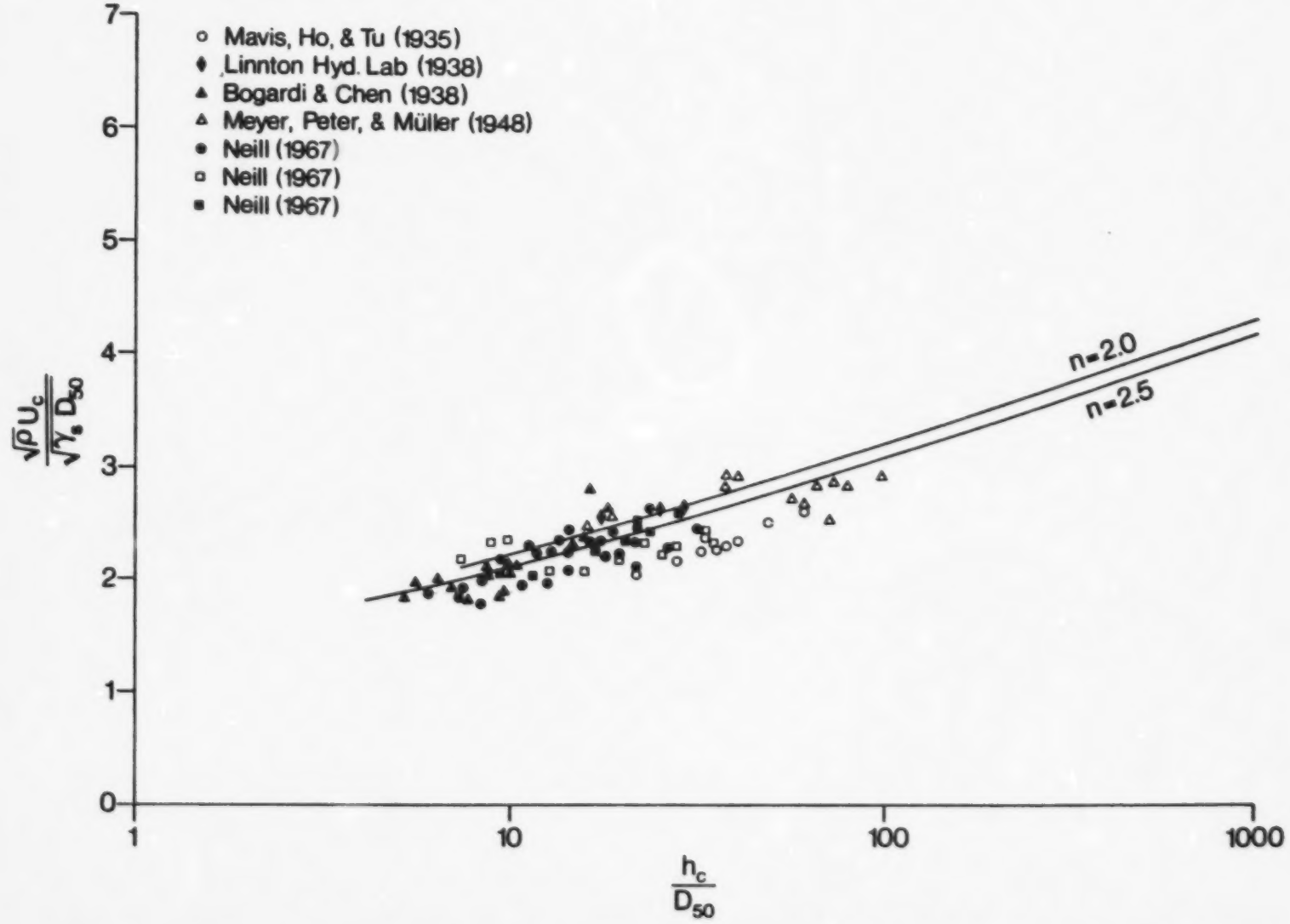

Figure 3 COMPARISON OF VELOCITY EQUATION WITH EXPERIMENTAL DATA FOR DIFFERENT VALUES OF n

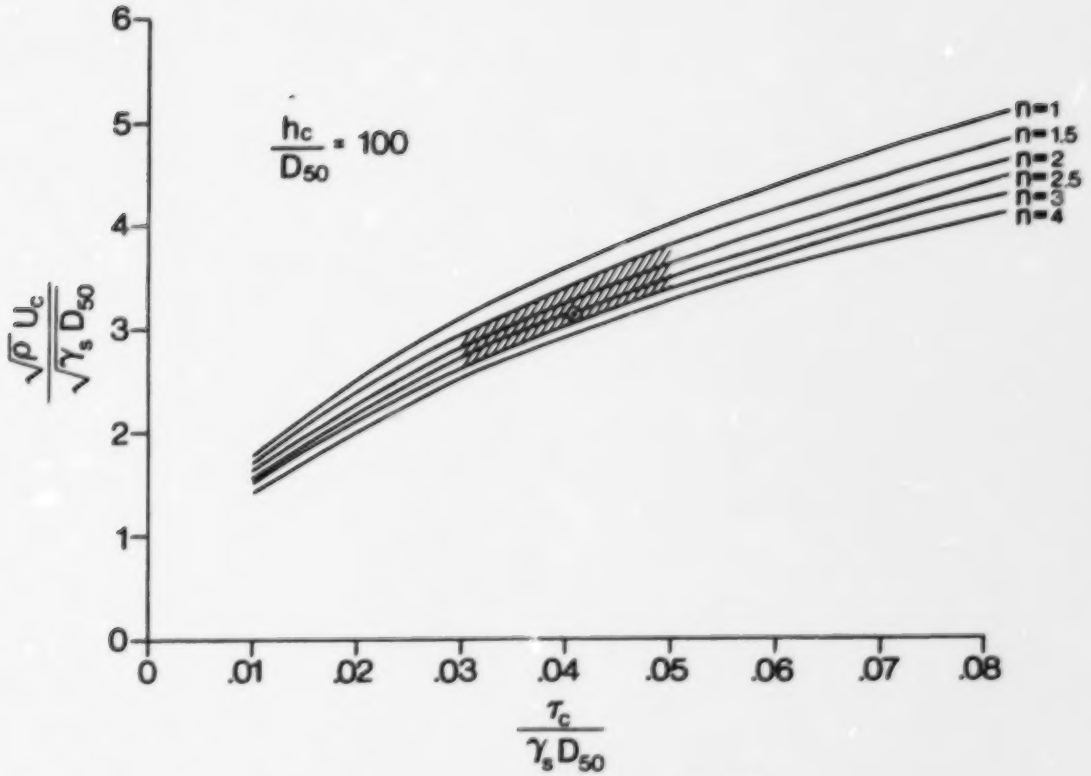

Figure 4 EFFECT OF $\frac{\tau_c}{\gamma_s D_{50}}$ AND n ON $\frac{\sqrt{\rho}\,U_c}{\sqrt{\gamma_s D_{50}}}$

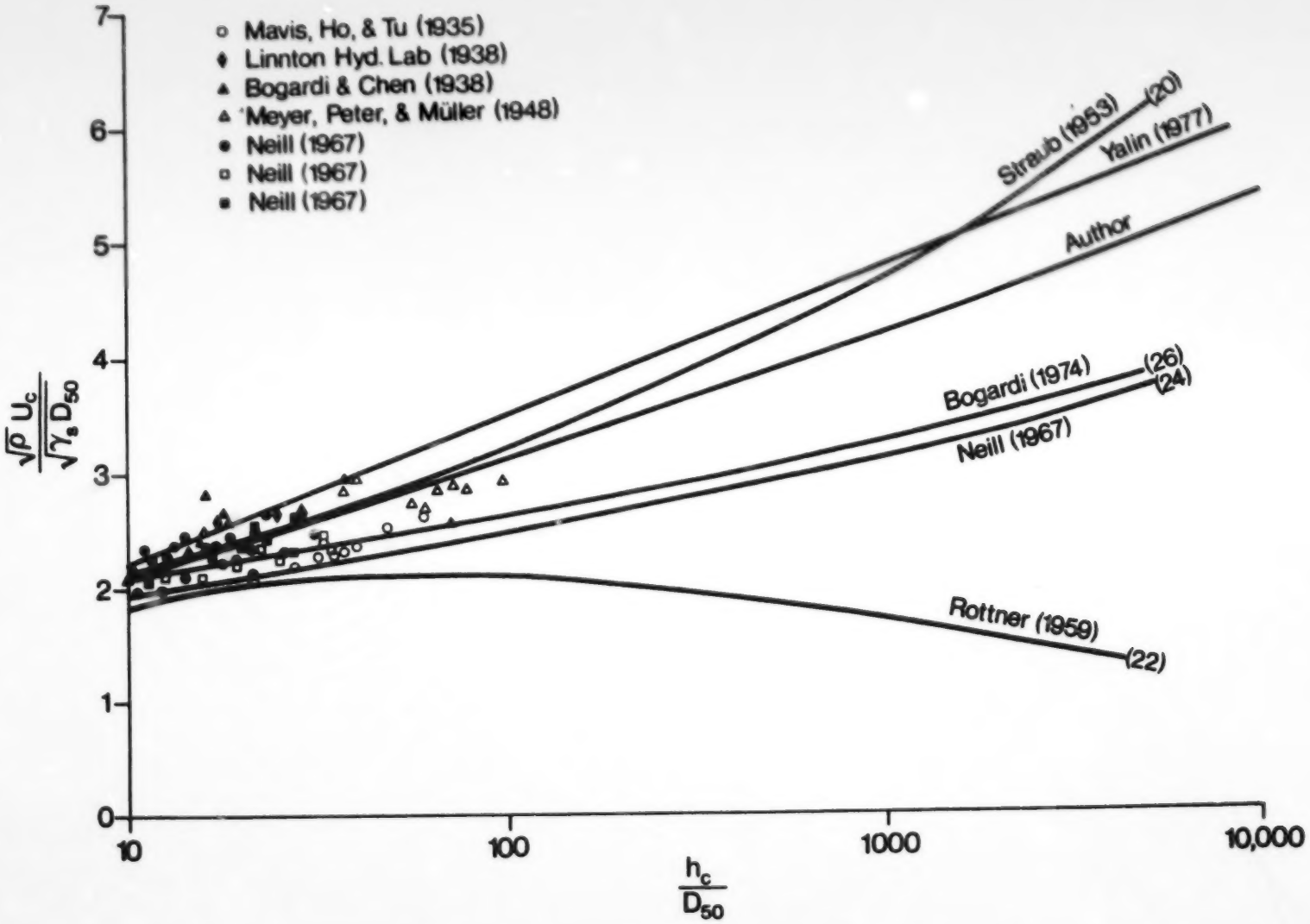

Figure 5 COMPARISON OF CRITICAL VELOCITY EQUATIONS

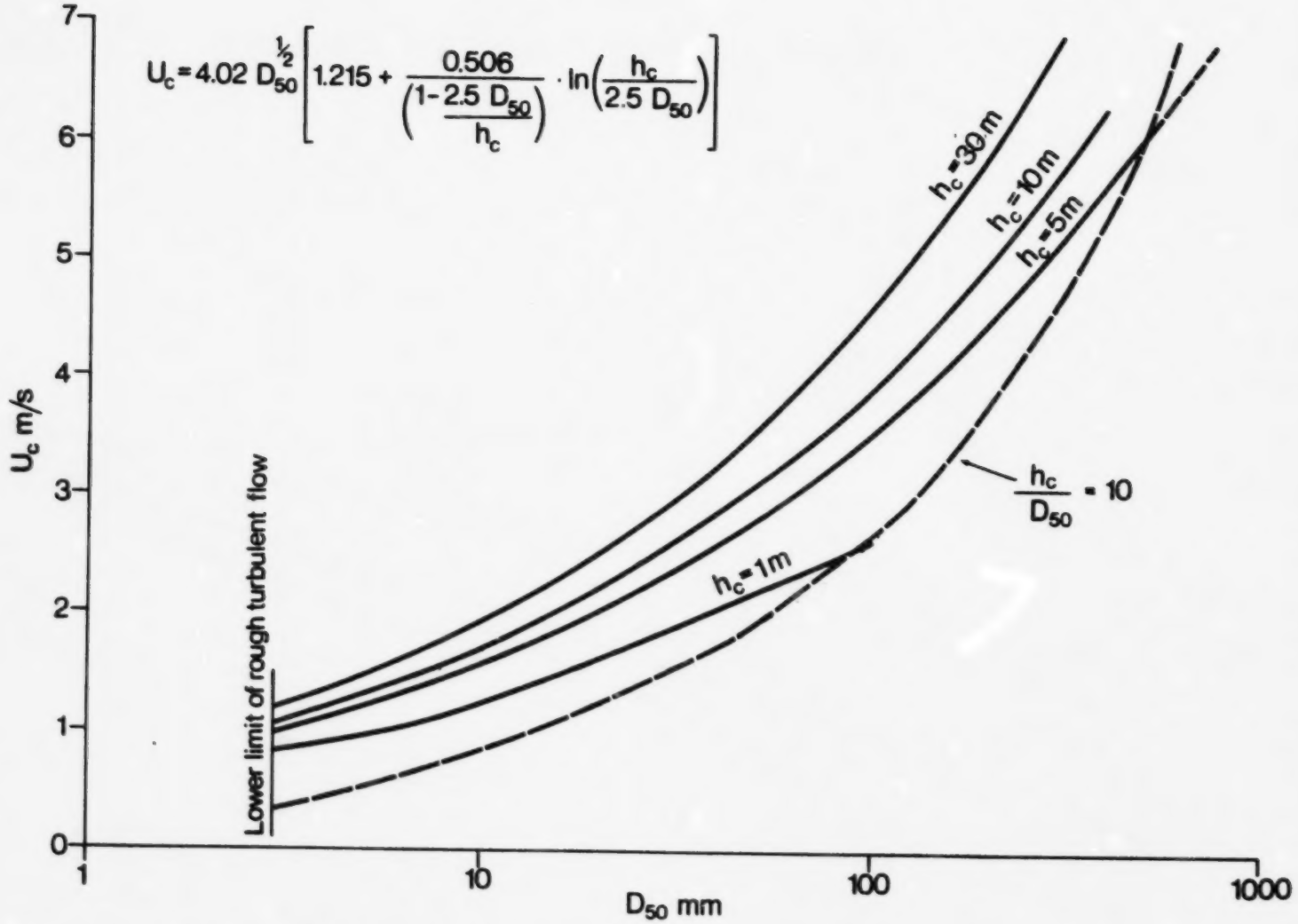

Figure 6 CURVES OF CRITICAL FLOW VELOCITY WHEN $\rho_s/\rho = 2.65$

POOR

QUALITY

ORIGINAL